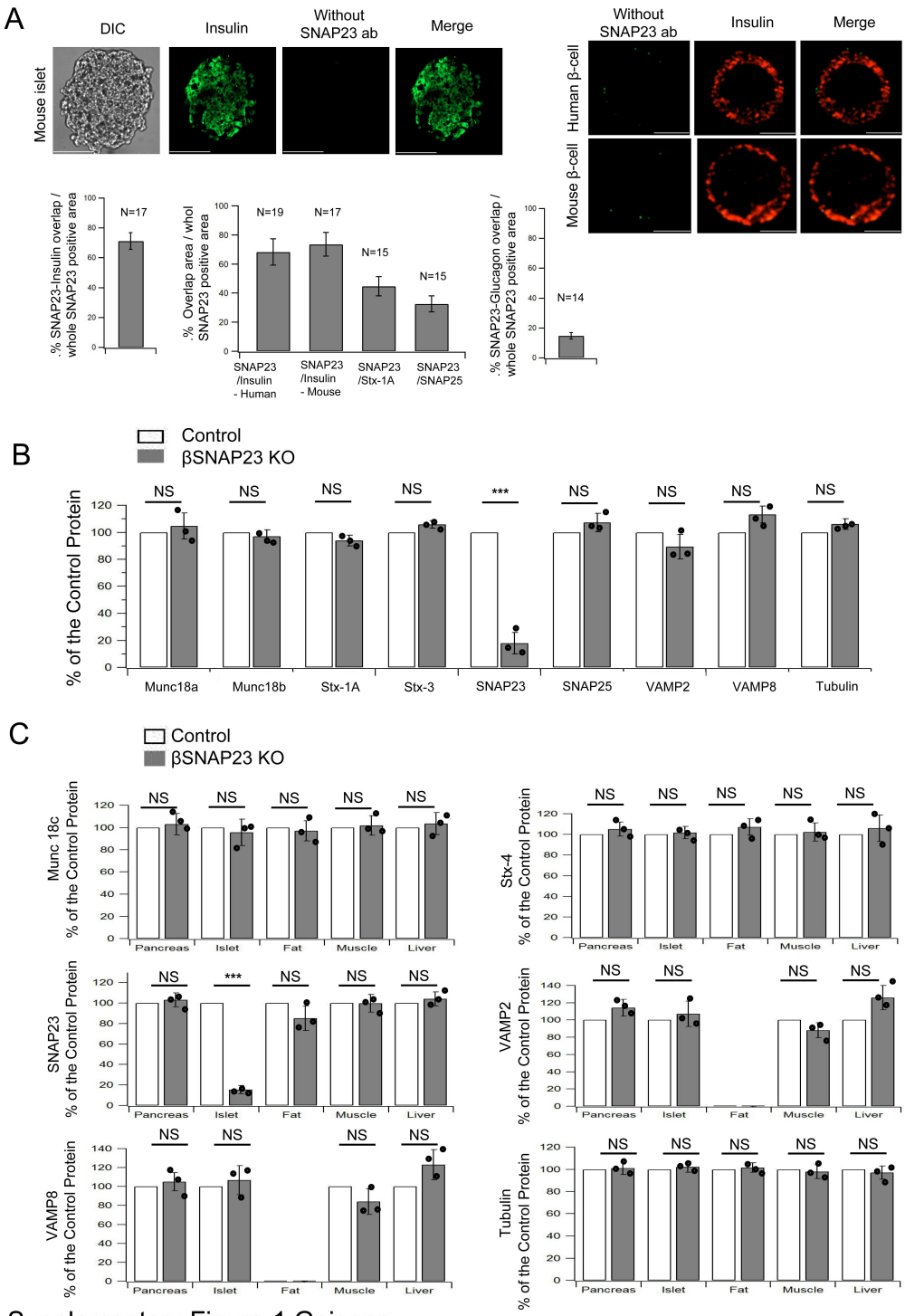

Supplementary Figure-1 Gaisano

Supplementary Figure 1. (**A**) *top left* **and** *top right* SNAP23 antibody controls, that is without primary SNAP23 antibody. This corresponds to Fig. 1A and 1B. Scale bar: 5 µm. (*bottom left):* Quantification of Fig 1A, 1B and 1C. The overlapping areas were normalized to the whole SNAP23 positive area and presented as a percentage. **(B)** Analysis of Fig 1F, N=3. **(C)** Analysis of Fig 1G, N=3.

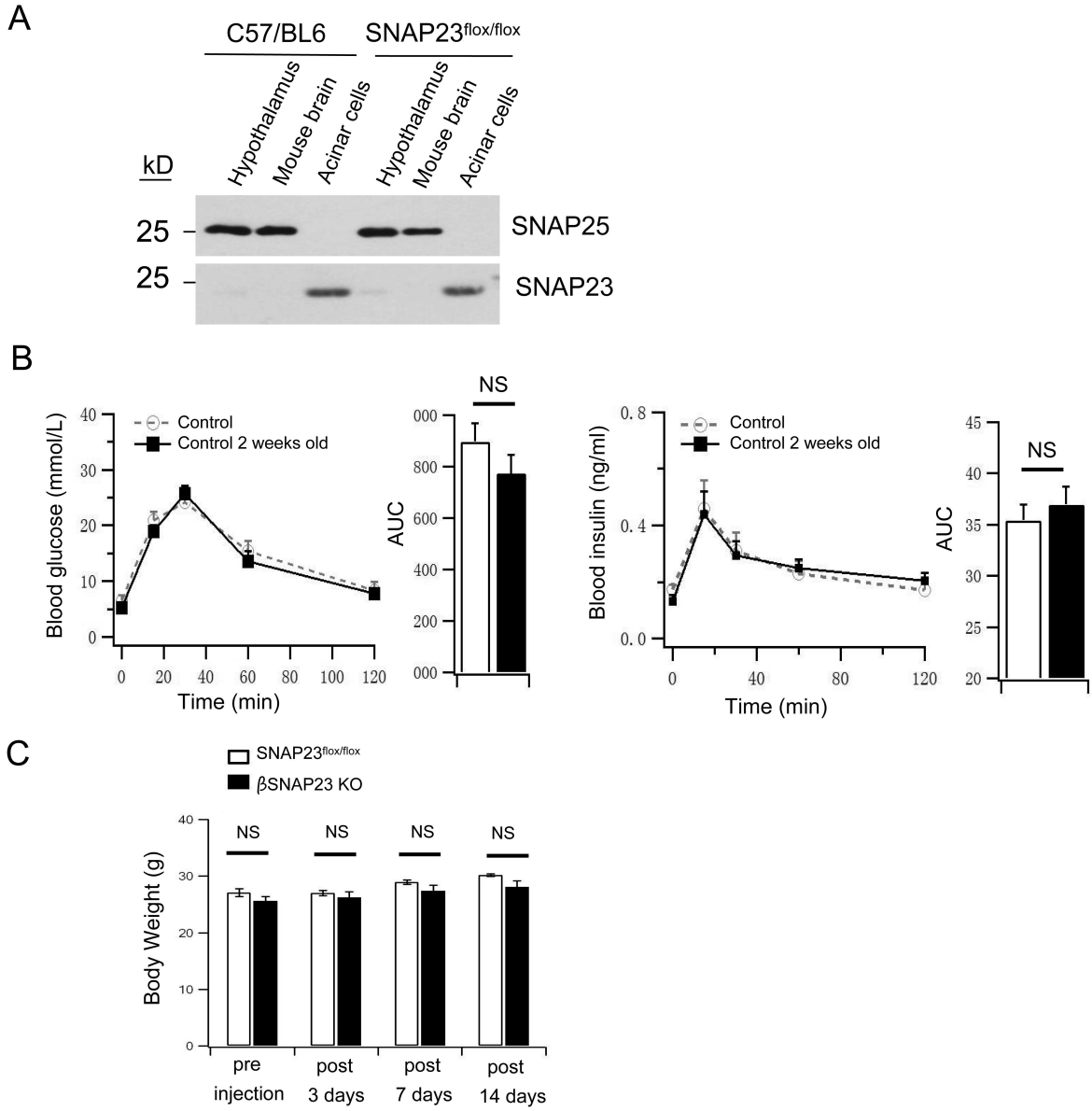

Supplementary Figure-2 Gaisano

Supplementary Figure 2 (A) Hypothalami were isolated from C57/BL6 mice and SNAP23$^{flox/flox}$ mice to determine the protein levels of SNAP25 and SNAP23. Mouse brain and acinar cell lysates were loaded as positive and negative controls. Shown are representative of the results from two separate experiments. **(B)** IPGTT performed on 8-10 weeks SNAP23$^{flox/flox}$ mice (no virus Control, N=11) at time 0 and at 2 weeks older, to match the AAV8-RIP1-Cre virus-treated mice in Fig. 2A (N=11) before virus treatment and 2 weeks after, showing no change in glucose homeostasis (*left*: glucose, *right*: insulin). **(C)** Weights were compared between the βSNAP23KO and age-matched no virus treatment SNAP23$^{flox/flox}$ mice, which showed no differences, indicating that βSNAP23 KO did not affect body weight. N=11. This result matches Fig. 2C.

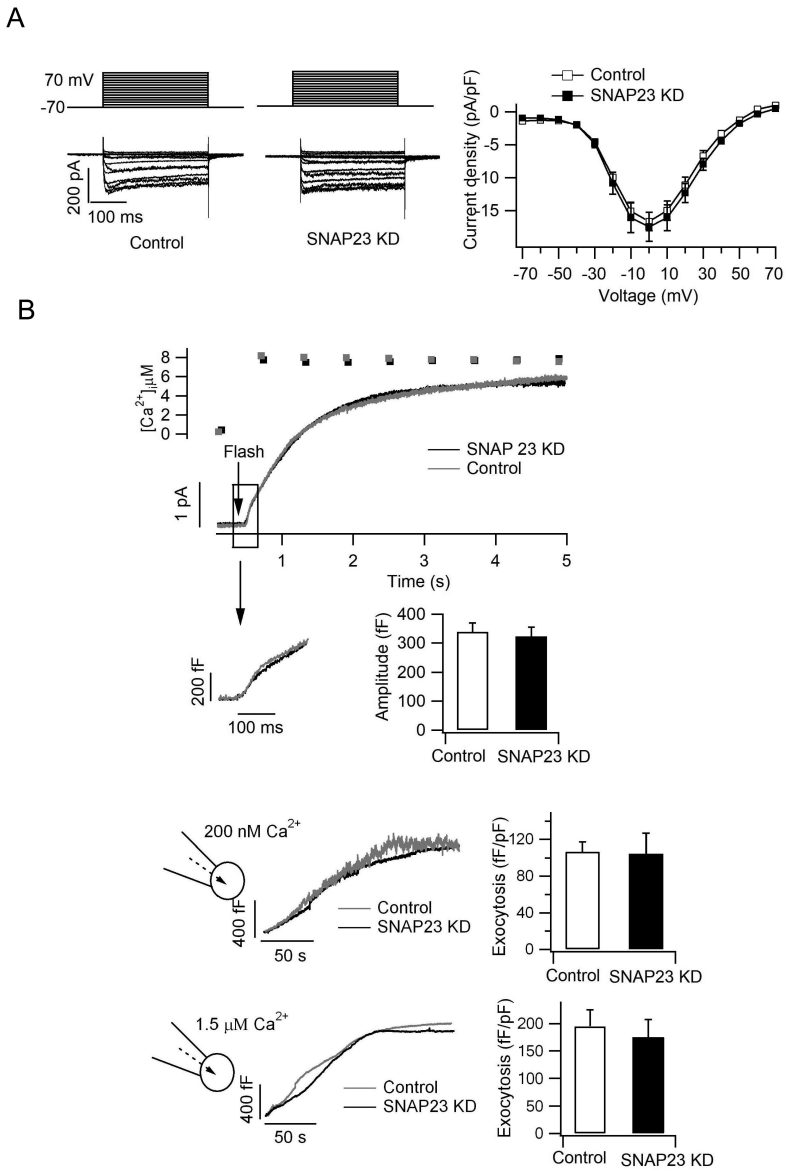

Supplementary Figure-3 Gaisano

Supplementary Figure 3 SNAP23-KD of human islet β-cells did not affect Ca_v channel currents or Ca^{2+} sensitivity of exocytosis. (**A**). *Left*, Representative traces showing Ca_v currents recorded in whole-cell mode from -70 to 70 mV with 10-mV increment from control and SNAP23-KD human β-cells. *Right*, Current-voltage relationship of Ca_vs from control (n=11) and SNAP23-KD (n=11) β-cells. Currents were normalized to cell capacitance to yield current density. Values are mean ± SEM. **(B)** *top:* Exocytosis was elicited by flash photolysis and was monitored by whole-cell membrane capacitance measurement. Averaged $[Ca^{2+}]_i$ and capacitance change from Control (gray, n=11) and SNAP23-KD (black, n=11) cells. Arrow indicates the flash time. *Middle:* Averaged amplitudes of the highly calcium-sensitive pool (HCSP) from Control and SNAP23-KD cells respectively. Values represent the Mean ± SEM. *Bottom:* Whole-cell capacitance change recorded during direct application of 200 nM or 1.5 μM free Ca^{2+} via patch pipette into control and SNAP23-KD human β-cells. *Right*: Average capacitance increments in control and SNAP23-KD cells at 200 s following initiation of Ca^{2+} infusion and normalized to initial cell size.

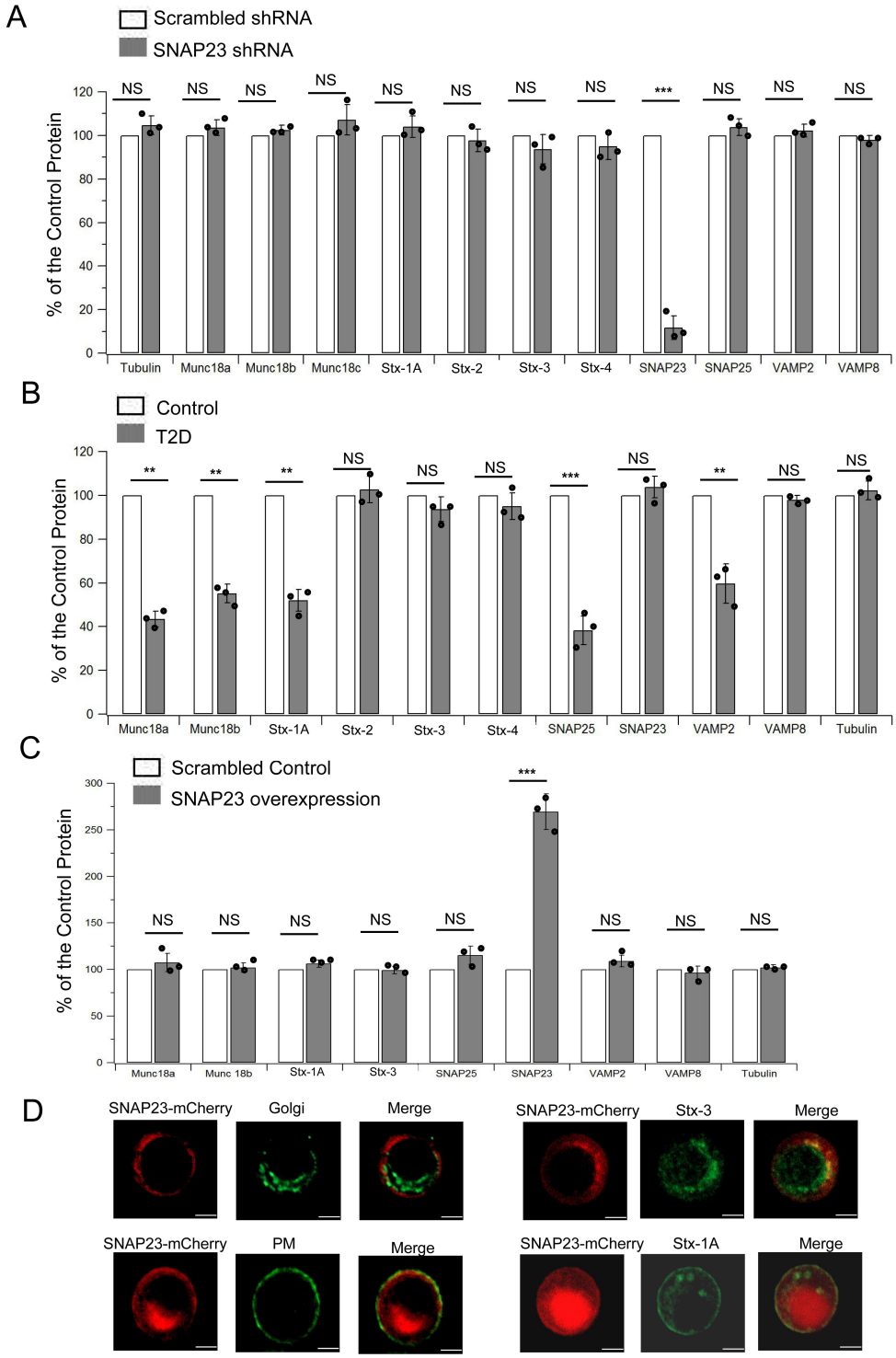

Supplementary Figure-4 Gaisano

Supplementary Figure 4 (A) Analysis of Fig 4A *right*, N=3. **(B)** Analysis of Fig 5A, N=3. **(C)** Analysis of Fig 6A, N=3. **(D)** Single human pancreatic β-cells showing the exogenously overexpressed SNAP23-mCherry did not just remain in the Golgi (GM-130 antibody, *left top*) but mostly surfaced to the PM where it partially co-localized with PM marker Phalloidin (*left bottom*) and SNARE proteins Stx-1A (*right bottom*) and Stx-3 (*right top*). Scale bar: 5 µm.

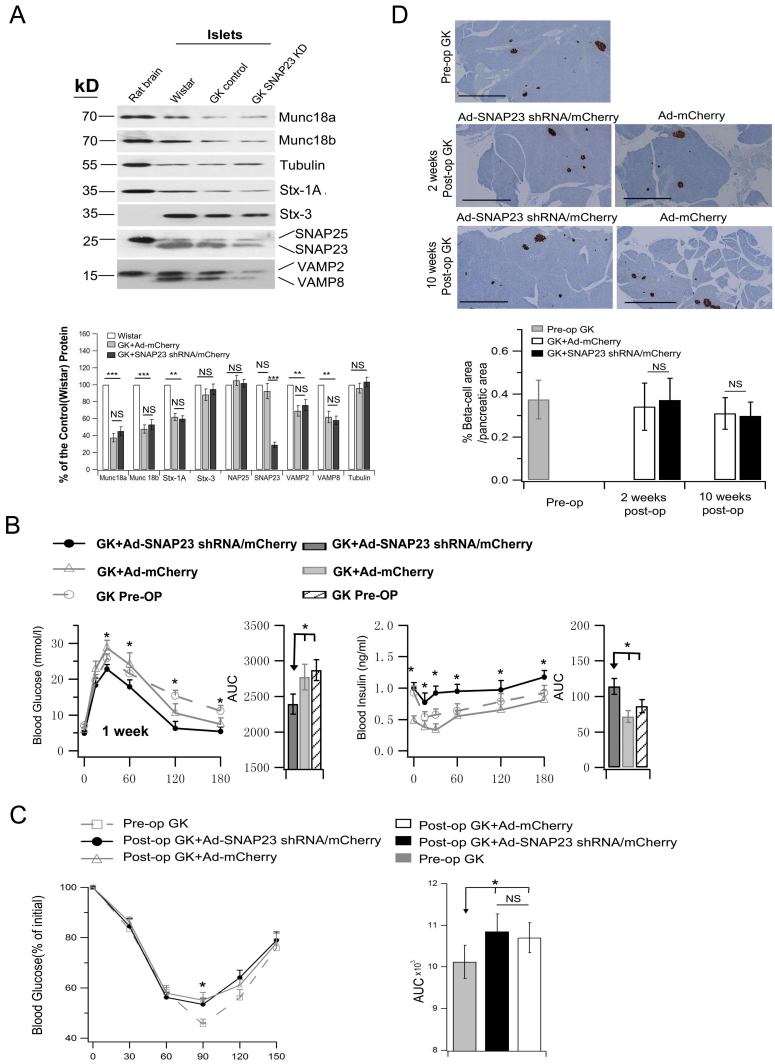

Supplementary Figure-5 Gaisano

Supplementary Figure 5 Pancreatic SNAP23 depletion in GK rats does not alter other islet exocytotic proteins, insulin tolerance or islet mass. Ad-SNAP23 shRNA/mCherry (6.6×10^9 PFU) vs Ad-mCherry (as control, same dose) was infused via pancreatic duct into GK rats. **(A)** Western blots analysis of SM and SNARE proteins of Ad-SNAP23 shRNA/mCherry and Ad-mCherry-transduced GK rat islets. Rat brain and Wistar rat islets are positive controls. *top* Data shown is representative of 3 sets of experiments. *Bottom*, densitometric analysis of SNAP23-KD GK islets compared to Ad-eGFP-transduced GK rat islets and Wistar islets (N=3). Other proteins showed no change after SNAP23 knockdown. **(B)** Comparison of pre-op and post-op IPGTTs. IPGTTS performed pre-op and post-op at 1 week showed no change between Ad-mCherry treatment and pre-op levels, with both being worse than after Ad-SNAP23 shRNA/mCherry treatment. Ad-SNAP23 shRNA/mCherry: N=6, Ad-mCherry control: N=6, Pre-op group: N=12. This study was to match Fig. 7. **(C)** IPITTs performed on 14 weeks old GK rats before the operation (N=11) vs 10 weeks post-op after pancreatic ductal infusion of Ad-SNAP23 shRNA/mCherry (24 weeks old, N=5) vs 10 weeks post-op GK rats with Ad-mCherry (24 weeks old, N=5). *Left*: Blood glucose results shown as percentages of initial levels. *Right*: AUCs encompassing 150 min of the IPITT. **(D)** *In vivo Ad*-SNAP23 shRNA treatment of GK rats did not alter islet β-cells mass. *Top***,** Insulin-immuno-stained pancreatic sections (scale bars represent 1000 μm). *Bottom*, Insulin-positive β-cell area per pancreatic area ratios. N=12 for each group from 4 independent experiments.

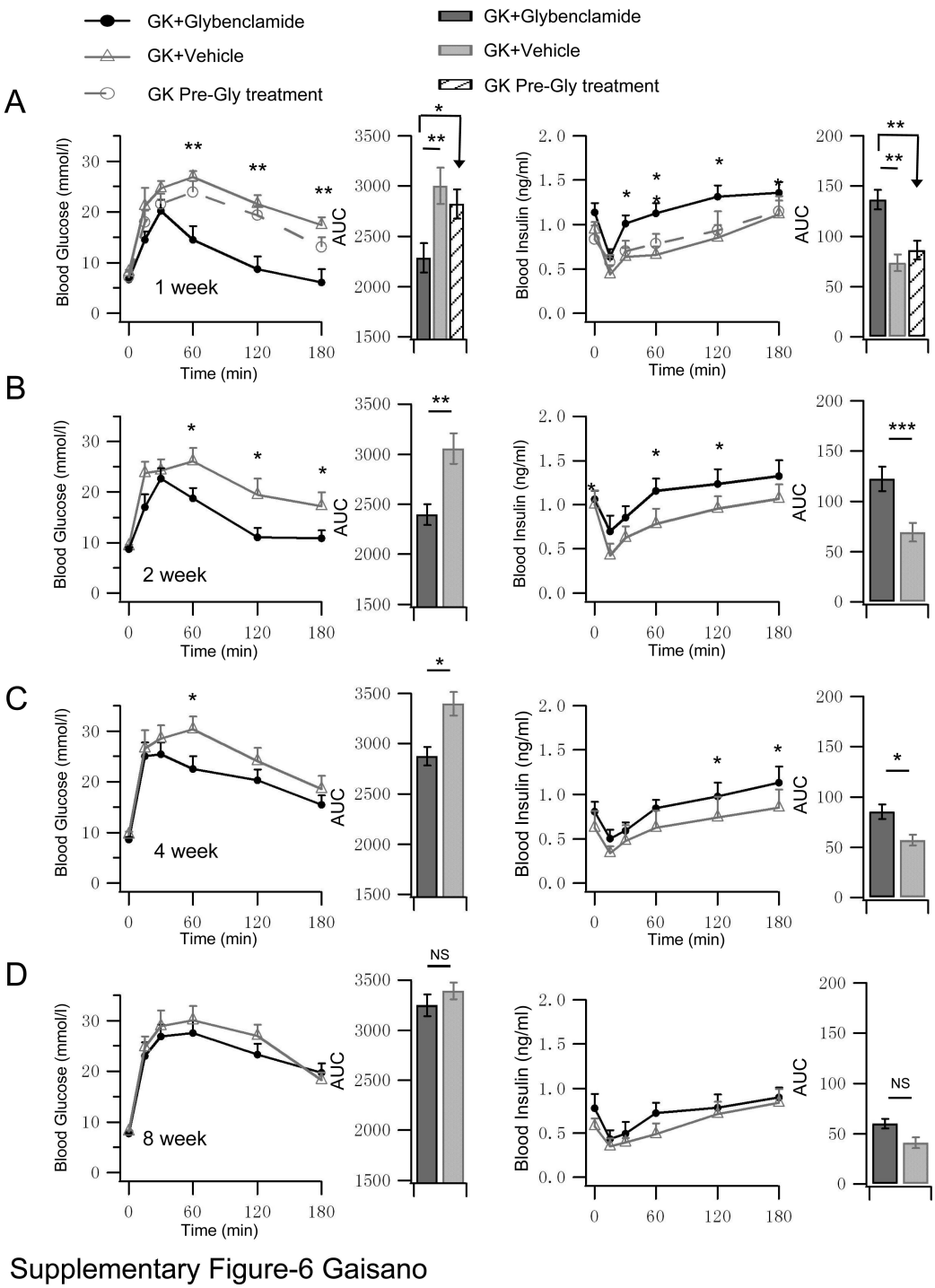

Supplementary Figure 6 Glybenclamide vs vehicle control was given to GK rats. IPGTTs (blood glucose and insulin levels obtained) were performed pre-treatment and post-treatment at 1 **(A)**, 2 **(B)** 4 **(C)** and 8 weeks **(D)**. This was to match Fig. 7, showing the vehicle control. Graphs on the right show AUCs encompassing 180 min of the IPGTTs. Glybenclamide pre-treatment: N=11; Glybenclamide treatment: N=6; Vehicle group: N=4.

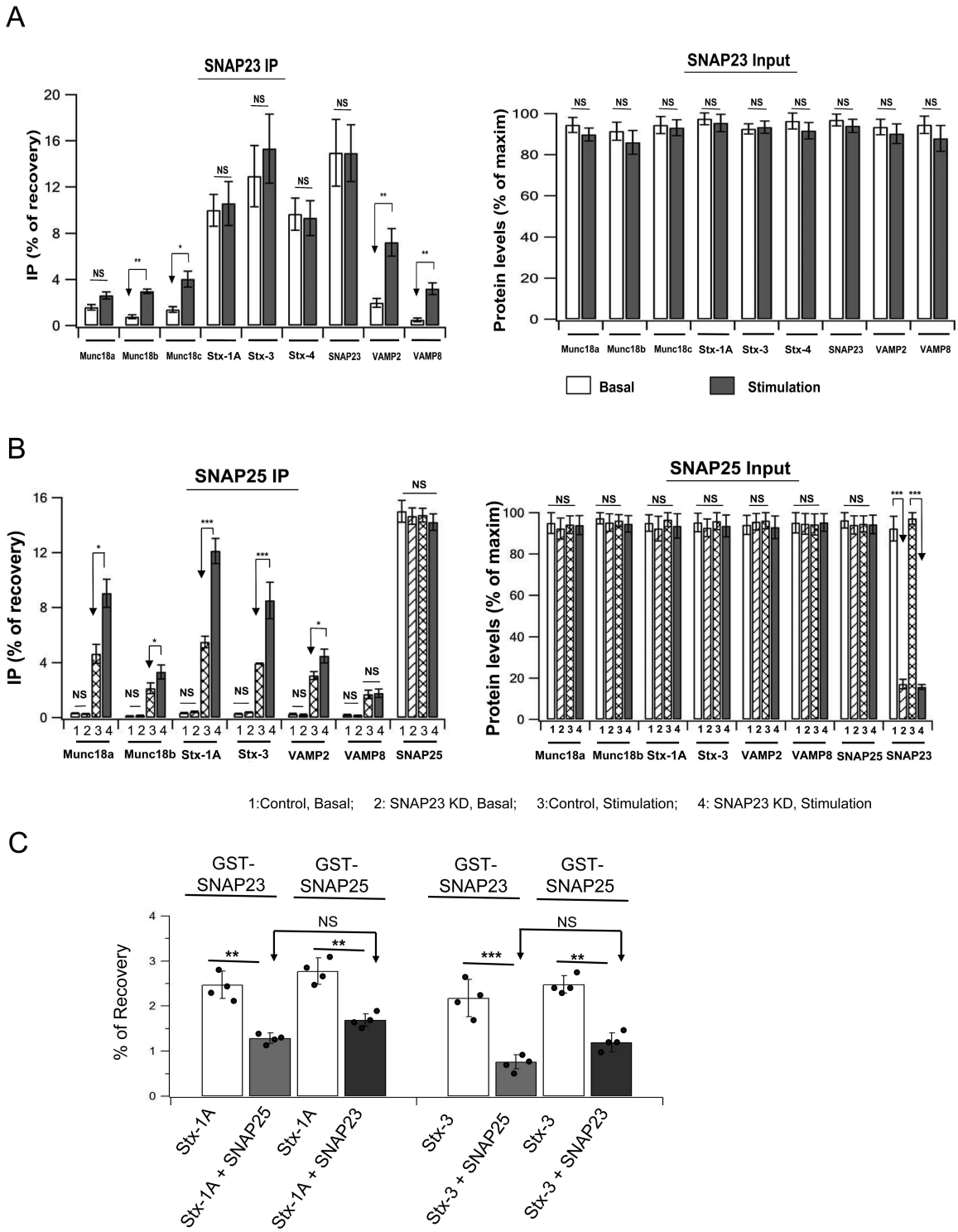

Supplementary Figure-7 Gaisano

Supplementary Figure 7 Analyses of Fig. 8, with **(A)** matching Fig. 8A (N=3), **(B)** matching Fig. 8B (N=3), and **(C)** matching Fig. 8C (N=4).

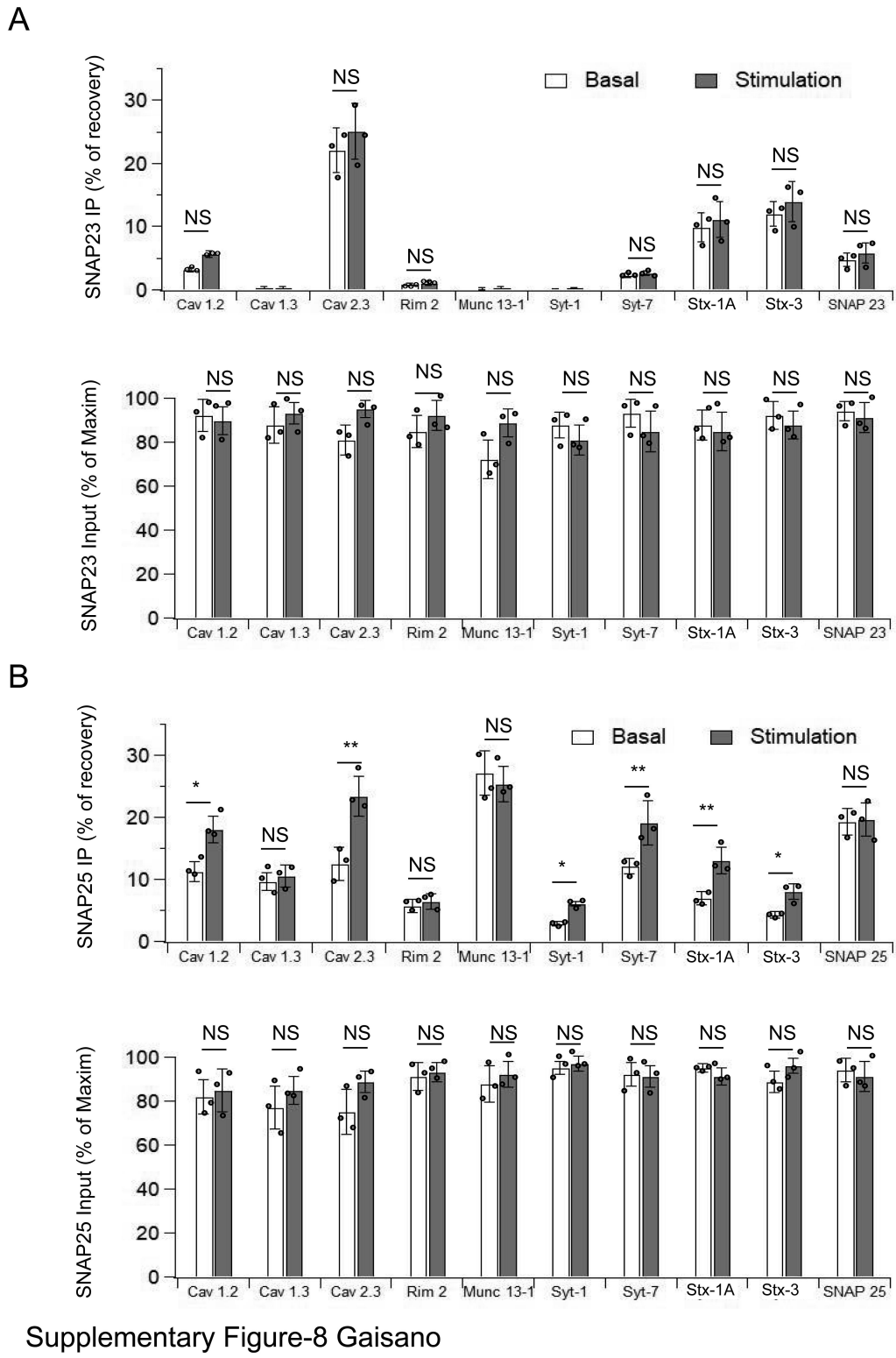

Supplementary Figure-8 Gaisano

Supplementary Figure 8 Analyses of Fig. 8D and 8E, with **(A)** matching Fig. 8D (N=3), **(B)** matching Fig. 8E (N=3).

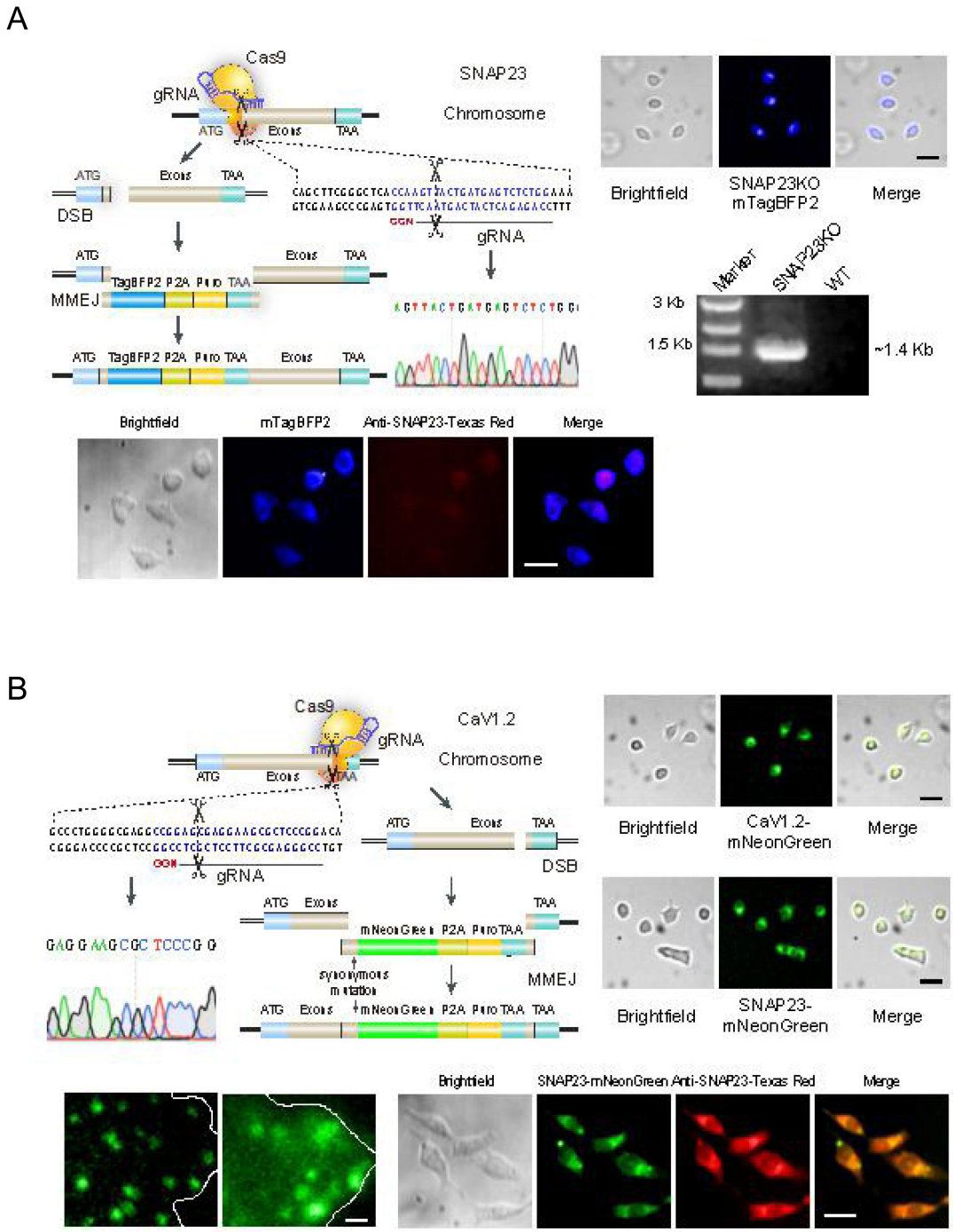

Supplementary Figure-9 Gaisano

Supplementary Figure 9 MMEJ-mediated knock-out at the SNAP23 locus (**A**) and knock-in at the $Ca_v1.2$ and SNAP23 locus (**B**) were performed using the method described by Sakuma *et al.*(54) **A** *top left*, Simplified schematic of MMEJ-mediated knock-out of SNAP23 in INS-832/13 cells. The gRNA cutting site was chosen to be immediately downstream of the start codon for SNAP23, and the double-stranded break (DSB) repaired with the sequence of mTageBFP2-Puromycin-stop codon TAA by microhomology-mediated end-joining (MMEJ) would disrupt the protein reading frame and then generate the knock-out. **A** *top right***,** Representative fluorescence images of SNAP23 knock-out (mTagBFP2) in INS-832/13 cells by MMEJ-mediated

knock-out. Scale bar, 20 μm. **A** *bottom right*, Detection of the SNAP23 knock-out mutation using PCR products amplified the indicator sequence of mTagBFP and Puromycin from genomes. The band indicates our knock-out strategy successfully replaced the endogenous gene of SNAP23 with mTagBFP2. **A** *bottom left***,** Immunofluorescence analysis of SNAP23 knock-out clone in INS-832/13 cells. SNAP23 was absent in mTagBFP2-indicated knock-out cells. Red, anti-SNAP23-Texas Red. Scale bar, 20 μm. **B** *top left***,** Simplified schematic of MMEJ-mediated knock-in at the $Ca_v1.2$ locus. The cutting site was chosen near the stop codon at $Ca_v1.2$, and the DSB is repaired with the sequence of mNeonGreen–Puromycin by MMEJ. **B** *top right***,** Representative fluorescence images of $Ca_v1.2$ knock-in (mNeonGreen) in INS-832/13 cells by MMEJ-mediated knock-in. Scale bar, 10μm. **B** *middle right*, Representative fluorescence images of SNAP23 knock-in (mNeonGreen) in INS-832/13 cells by MMEJ-mediated knock-in, which we employed similar strategy with the knock-out of $Ca_v1.2$. Scale bar, 20 μm. **B** *bottom left*, Live-cell imaging of MMEJ-mediated endogenous tagging of $Ca_v1.2$ gene with mNeonGreen. The endogenous $Ca_v1.2$ (*left*) is distributed across the plasma membrane as discrete hotspots which is quite different from the location of overexpressed Cav1.2 (*right*)shown as larger hotspots or clusters. Scale bar, 1 μm. **B** *bottom right*, Immunofluorescence analysis of SNAP23 knock-in clone in INS-832/13 cells under confocal microscopy. Green, endogenous SNAP23 was labelled with mNeonGreen. Red, anti-SNAP23-Texas Red. Scale bar, 20 μm.

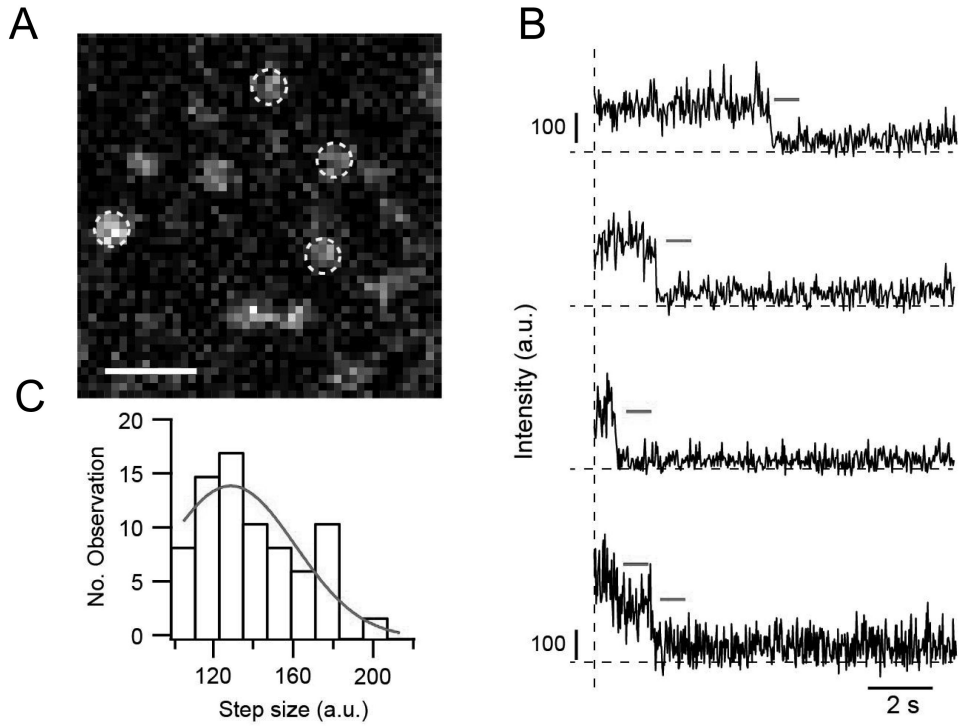

Supplementary Figure-10 Gaisano

Supplementary Figure 10 Single molecules in fixed INS-832/13 cells. (**A**) INS-832/13 cells transiently transfected with SNAP25-mScarlet and then fixed by 4% Paraformaldehyde (PFA). Image is an average of 5 sequential frames. (Scale bar, 1 μm.) (**B**) Representative stepwise downward photobleaching traces of SNAP25-mScarlet. The intensity was measured and averaged over a 3×3 region, as yellow circles indicated in **a**. Dashed horizontal lines indicate the background. (**C**) Histogram of step size. The step size was calculated by the average intensity difference between before and after bleaching.

82

83 **Supplemental Table 1**

84 **Table S1. Information on pancreatic islet donors**

Donor Category	Age (yr)	Sex	BMI (kg/m^2)	HbA1c (%)	Isolation ID	Date of Shipment	Medical treatment
T2D Donors	55	F	27.5	9.2	R107	18/11/2014	No medication, uncontrolled
	75	M	26.4	6.3	R093	25/08/2014	Metformin, no insulin
	47	F	35	5.9	R078	01/05/2014	Diet controlled
	53	F	36	10.3	R057	03/06/2013	Metformin, no insulin
	74	F	22	6.1	R054	08/04/2013	No record of medication
Normal Donors	52	M	22.4	5.9	R106	13/11/2014	
	42	M	25	5.9	R104	20/10/2014	
	34	F	26	NA	R99	29/09/2014	
	61	M	26	5.4	R098	25/09/2014	
	53	F	28	5.4	R096	11/09/2014	
	65	M	28	NA	R091	28/07/2014	
	63	M	26	5.5	R076	28/04/2013	
	32	F	31	5.8	R056	10/06/2013	
	48	F	24	5.8	R052	02/04/2013	
	72	F	22	6.1	R050	12/02/2013	

85